

2014

Candidate chromosome 1 disease susceptibility genes for Sjogren's syndrome xerostomia are narrowed by novel NOD.B10 congenic mice

P. K. A. Mongini

Zucker School of Medicine at Hofstra/Northwell

J. M. Kramer

Northwell Health

T. Ishikawa

H. Herschman

D. Esposito

Follow this and additional works at: <https://academicworks.medicine.hofstra.edu/articles>



Part of the [Medical Molecular Biology Commons](#)

Recommended Citation

Mongini P, Kramer J, Ishikawa T, Herschman H, Esposito D. Candidate chromosome 1 disease susceptibility genes for Sjogren's syndrome xerostomia are narrowed by novel NOD.B10 congenic mice. . 2014 Jan 01; 153(1):Article 2861 [p.]. Available from: <https://academicworks.medicine.hofstra.edu/articles/2861>. Free full text article.

This Article is brought to you for free and open access by Donald and Barbara Zucker School of Medicine Academic Works. It has been accepted for inclusion in Journal Articles by an authorized administrator of Donald and Barbara Zucker School of Medicine Academic Works. For more information, please contact academicworks@hofstra.edu.



Published in final edited form as:

Clin Immunol. 2014 July ; 153(1): 79–90. doi:10.1016/j.clim.2014.03.012.

Candidate chromosome 1 disease susceptibility genes for Sjogren's syndrome xerostomia are narrowed by novel NOD.B10 congenic mice

Patricia K. A. Mongini^a and Jill M. Kramer^{a,1}

Tomo-o Ishikawa^{b,2} and Harvey Herschman^b

Donna Esposito^c

^aThe Feinstein Institute for Medical Research North Shore-Long Island Jewish Health System 350 Community Drive Manhasset, NY 11030

^bDavid Geffen School of Medicine at UCLA 341 Boyer Hall (MBI) 611 Charles E. Young Drive East Los Angeles, CA 90095

^cCharles River Laboratories, Genetic Testing Services 185 Jordan Road, Troy, NY 12180

Abstract

Sjogren's syndrome (SS) is characterized by salivary gland leukocytic infiltrates and impaired salivation (xerostomia). *Cox-2* (*Ptgs2*) is located on chromosome 1 within the span of the *Aec2* region. In an attempt to demonstrate that COX-2 drives antibody-dependent hyposalivation, NOD.B10 congenic mice bearing a *Cox-2**flox* gene were generated. A congenic line with non-NOD alleles in *Cox-2*-flanking genes failed manifest xerostomia. Further backcrossing yielded *disease-susceptible* NOD.B10 *Cox-2**flox* lines; fine genetic mapping determined that critical *Aec2* genes lie within a 1.56 to 2.17 Mb span of DNA downstream of *Cox-2*. Bioinformatics analysis

© 2014 Elsevier Inc. All rights reserved.

Address correspondence to: Dr. Patricia Mongini Laboratory of B Cell Biology The Feinstein Institute for Medical Research 350 Community Drive Manhasset, NY 11030 TEL: 516-562-3442 FAX: 516-562-1011 pmongini@nshs.edu.

¹Present address: School of Dental Medicine Department of Oral Biology 3435 Main Street 211 Foster Hall Buffalo, NY 14214 jkramer@buffalo.edu

²Present address: TransGenic Inc. Kobe Research Center 7-1-14 Minatojimaminami-machi, Chuo-ku, Kobe-shi, Hyogo 650-0047 Japan tishikaw@xf7.so-net.ne.jp

pmongini@nshs.edu; tel: (516)-560-3442

jkramer@buffalo.edu; tel: (716) 829-2551

tishikaw@xf7.so-net.ne.jp

HHerschman@mednet.ucla.edu; tel: (310) 825-8735

Donna.Esposito@crl.com; tel: (518)286-0016

Author roles: *PKAM*: conceived, designed and coordinated the project; performed experiments, including salivation analysis, salivary gland excision and histological analysis; bioinformatics and statistical analyses; and drafted the original manuscript. *JK*: provided guidance in salivary gland excision and identification of foci; executed a blind assessment of size and frequency of foci; and helped write the manuscript; *TI* and *HH*: generated original mice with floxed *Cox-2* and provided founder mice used for present backcrossing; provided assistance in primers; and helped analyze data and write the manuscript; *DE*: coordinated all genetic testing performed during MAX-BAX® speed congenic breeding at Charles River Laboratories; identified and directed the testing of additional SNP markers for fine mapping; and helped write the manuscript. All authors read and approved the final manuscript.

Publisher's Disclaimer: This is a PDF file of an unedited manuscript that has been accepted for publication. As a service to our customers we are providing this early version of the manuscript. The manuscript will undergo copyediting, typesetting, and review of the resulting proof before it is published in its final citable form. Please note that during the production process errors may be discovered which could affect the content, and all legal disclaimers that apply to the journal pertain.

revealed that susceptible and non-susceptible lines exhibit non-synonymous coding SNPs in 8 protein-encoding genes of this region, thereby better delineating candidate *Aec2* alleles needed for SS xerostomia.

1. INTRODUCTION

Sjogren's syndrome (SS) is an autoimmune disorder characterized by severely impaired salivary and lachrymal gland function, multiple systemic effects, and a relatively high incidence of B cell lymphoma [1, 2]. Affected salivary glands show leukocytic infiltrates characterized by prominent T cell and B cell foci, occasional germinal centers, and autoantibody-producing plasma cells [1].

In both humans and mice with SS, there is strong evidence of a B cell pathogenic role. SS development is highly linked to overexpression of BAFF [3], a potent B cell survival factor. Furthermore, in SS-vulnerable NOD mice, B cells are required for age-related hyposalivation (xerostomia) [4, 5], and in humans with SS, a therapeutic response to B cell-depleting Rituximab is reported [6]. AutoAbs to several intracellular e.g. SS-A/Ro and SS-B/La, are characteristically generated in this disorder [7, 8]. Xerostomia in both NOD mice [9, 10] and SS-afflicted humans [11, 12] is linked to pathogenic, class-switched IgG antibodies that target the M3R muscarinic acetylcholine receptor on salivary gland cells, impairing acinar cell function. Nonetheless, the cause of xerostomia is undoubtedly multifactorial.

Th17 inflammatory cells represent a major subset within salivary gland T cell foci of SS-afflicted patients and mice [13]. Through synthesis of inflammatory IL-17 and other cytokines, Th17 cells influence the inflammatory state of the afflicted tissue [14] and promote the development of Ab-producing germinal centers [15]. The reason why Th17 cells accumulate in SS salivary glands is unclear but may involve heightened expression of critical cytokines and transcription factors needed for their development and/or expansion [16, 17]. In addition, it may involve inflammatory lipids, such as arachidonic acid-derived prostaglandin E2 (PGE2), given that the latter significantly augments Th17 cell expansion through several routes [18-20].

In humans, predisposition to SS appears to be multigenic [21] and in NOD (NOD.B10) mice, spontaneous SS development upon aging depends upon disease susceptibility alleles located in Chr 1 (*Aec2*) and Chr 3 (*Aec1*) [22, 23]. The genes whose allelic differences determine NOD susceptibility to SS remain unknown. Nevertheless, Nguyen et al. have gained insights through linking their observations on the disease process with genes located in narrowed *Aec1* and *Aec2* regions following the breeding of NOD disease susceptibility genes onto the C57BL6 genetic background [23, 24]. Genes of possible interest within the 2006-mapped *Aec1* locus of B6.*Aec1*/2 mice encoded IL-2, IL-7, carbonic anhydrase, and retroviral integration sites [24] while genes of possible interest within the 2008-mapped *Aec2* locus fell into groups involving endogenous viruses and oncogenes, Fas/FasL-associated apoptosis, Th17-associated activities, and lipid/lipoprotein homeostasis [24].

Recently, we undertook efforts to introduce a floxed *Cox-2* (*Ptgs2*) gene onto the NOD.B10 genetic background for the future purpose of investigating whether B cell-specific COX-2 expression was important for xerostomia development. This was warranted given (a) strong evidence that COX-2 and downstream PGE2 have a role in regulating the production of class-switched Abs [25, 26], (b) evidence that cycling B lymphocytes show elevated synthesis of several PGE2 axis proteins, as well as PGE2 [27, 28], and (c) the above cited influences of PGE2 on Th17 expansion.

In the present report, we identify a NOD.B10 *Cox-2flox-expressing* congenic mouse line that failed to manifest age-related xerostomia, prior to introduction of Cre recombinase. Through genetic fine mapping, we show the NOD.B10 *Cox-2flox* congenic mouse exhibits a replacement of NOD alleles within a recently narrowed *Aec2* span [23] that includes the *Cox-2flox* allele and flanking Chr 1 genes from a SS non-susceptible genetic background. Importantly, we demonstrate that genetic alleles strongly influencing SS xerostomia lie within a significantly more narrowed span of this earlier *Aec2* locus. This latter insight came from identifying novel SS-susceptible mice with recombinations in the region following further backcrossing. In significantly narrowing the Chr 1 *Aec2* span influencing xerostomia, the study has better delineated the candidate disease susceptibility genes therein.

2. MATERIALS & METHODS

2.1 Mice and speed congenic breeding

This study was carried out in accordance with the Guide for the Care and Use of Laboratory Animals of the National Institutes of Health. The protocol was approved by the Institutional Animal Care and Use Committee (IACUC) of The Feinstein Institute for Medical Research (Project number: 2008-001). *NOD.B10Sn-H2^b/J*: Male and female mice were obtained from Jackson Labs (Bar Harbor, MA). *Cox-2flox/flox*: mice bearing a floxed *Cox-2* gene on a mixed 129/B6 background were developed and first described by Ishikawa and Herschman [29]. Insertion of LoxP sites into introns of the *Cox-2* gene has no effect on either baseline or induced COX-2 expression in mouse macrophages [30].

Male *Cox-2flox*⁺-bearing founders were crossed with NOD.B10 females and backcrossing the *Cox-2flox* gene continued on the NOD.B10 background, at Charles River Laboratories under contract with the Feinstein Institute. For the first backcross (BC) generation of the NOD.B10 *Cox-2flox*⁺ congenic lines, F1 females were crossed with male NOD.B10 mice to fix the Y chromosome as NOD genotype. Thereafter, all subsequent backcross generations were derived from crossing female NOD.B10 dames with males selected by speed congenic breeding and genetic testing [31] to possess (a) the *Cox-2flox* gene and (b) the greatest homology to NOD.B10 across all autosomal chromosomes. The genetic screen encompassed 104 microsatellite markers which scanned the 19 autosomal chromosomes at approximately ~ 15 cM intervals (MAXBAX® speed congenic breeding; Charles River Laboratories). Additionally, at the second backcross generation, the genetic screen included a probe for the NOD.B10 MHC alleles. Typically three male mice from each generation with the greatest NOD homology were chosen for the next backcross to female NOD.B10 mice. After the N5 generation, additional fine mapping involved further microsatellite markers and single nucleotide polymorphism (SNP) markers that distinguished the NOD and

129 and B6 genetic backgrounds. The screen for the *Cox-2flox* gene involved testing tail-snip genomic DNA with primers for *Cox-2* intron 3 (forward): 5'-CTACTGGAGCAGAATGTCCTGTG-3' and Exon 4 (reverse): 5'-ATTGTAAGTAGGGTGGACTGTCAATCA-3' (floxed: ~ 500 bp band; wildtype: ~ 254 bp band; heterozygous: 500 bp + 254 bp). All genetic testing was performed at Charles River Laboratories (Troy, NY).

As the backcross generations were established, littermate mice of each generation which had been identified to lack the *Cox-2flox* allele were tested as wild-type positive controls for development of SS, together with NOD.B10 wild-type (WT) mice from Jackson Labs. C57BL/6J mice (Jackson Labs) were used as negative controls for SS disease. Prior to testing for salivation, mice had been aged at The Feinstein Institute to at least 5 months of age.

2.2 Bioinformatics analysis of mouse SNPs in *Cox-2* (*Ptgs2*) and proximal genes in *Aec2*

The Mouse Genome Database (MGD) [32] at the [Mouse Genome Informatics](http://www.informatics.jax.org) website, The Jackson Laboratory, Bar Harbor, Maine. World Wide Web (URL: <http://www.informatics.jax.org>) [Nov 2013] and the Mouse Phenome Database at the Jackson Laboratory (URL: <http://phenome.jax.org/>) [Jan 2014] were used for mapping microsatellite and SNP markers and for discerning comparative data on inbred strains: NOD/ShiLtJ, 129S1/SvImJ, and C57BL/6. (While the modified *Cox-2flox* gene is from the strain 129 background, a screen for C57BL/6 was included due to maintenance on a mixed 129/B6 background.) Each of the above strain designations were scanned for differing SNP alleles in the gene for *Cox-2* (*Ptgs2*) and protein-encoding genes mapped to later delineated *Aec2* regions A, B, and C.

2.3 Salivation Assays

Upon aging (5 mo), NOD.B10 mice of both ♂ and ♀ gender characteristically display hyposalivation [9, 33]. Salivation data were obtained by intraperitoneal (i.p.) injection with the muscarinic acetylcholine receptor agonist, pilocarpine (Sigma; St. Louis, MO) at 0.5 µg per gram body weight. Saliva was collected for a period of 10 minutes with a pipette, beginning at 2 minutes following pilocarpine injection, using restraint only with no anesthetic, as described by others [34]. Saliva was transferred into pre-weighed Eppendorf tubes, which were re-weighed and saliva amount computed as mg per gram mouse weight.

2.4 Assessment of mouse salivary gland histopathology

Submandibular glands from euthanized male and female mice (ranging from 6 to 18 months of age, as indicated) were excised, fixed in formalin, embedded in paraffin, sectioned, and stained with H&E. The presence of periductal or perivascular focal lymphocytic sialoadenitis (FLS) was evaluated by microscopy as previously described [35]. Briefly, the number of lymphocytic foci was quantified, where a focus represents 50 lymphocytes in a 4mm² area. The number of focus scores was normalized by dividing the number of foci by the average area examined for each treatment group, and by measuring the size of individual foci for each animal. All measurements were made using cellSens Standard software (Olympus).

2.5 Statistical Analysis

Statistical evaluations of measurements within distinctive mouse subgroups were performed with Excel software; expressed as mean \pm SEM; and assessed for significance using a Student's t test (unpaired; two-sided. Statistical significance was defined as a p value less than 0.05).

3.0 RESULTS

3.1 Mapping of recombination sites in novel NOD.B10 congenic mouse lines expressing *Cox-2flox*

A schematic of the speed-congenic backcrossing approach used to develop several NOD.B10 congenic lines expressing *Cox-2flox* is illustrated in Figure 1 (and detailed in Section 2.1). **Line A** was the first *Cox-2flox* congenic mouse line identified in the N5 generation of speed-congenic breeding (Table 1). These mice were determined to be > 99% of NOD genotype; they retained NOD alleles in all genes excepting those in a region of Chr 1 proximal to the floxed *Cox-2* gene (*Ptgs2*) and a distal portion of Chr 16 (devoid of known disease susceptibility genes). In the N6 generation, Chr 16 was fully NOD while Chr 1, similarly to the N5 generation, exhibited non-NOD alleles that included the span 133.44 Mb to 158.26 Mb from the Chr 1 centromere, at a minimum. The non-NOD Chr 1 interval includes the *Cox-2flox* gene itself (of strain 129 origin) [29] and proximal genes throughout the recently narrowed *Aec2* disease susceptibility region reported by Nguyen et al. to extend from D1Mit348 (133.44 Mb) through D1Mit268 (157.36 Mb) [23].

Cox-2flox **Line B** mice are derived from a further recombination within the *Aec2* region, first detected in the N6 generation of backcrossing *Cox-2flox* onto NOD.B10 wild-type females (Table 1). Fine mapping with microsatellite markers and selected SNP markers confirmed that these mice harbor non-NOD alleles in a shorter span extending from 133.44 Mb through 155.19 Mb from the Chr 1 centromere. Because additional fine mapping markers were unavailable, the *non-NOD* region may extend maximally from > 131.66 (outside the recently narrowed *Aec2* region [23]) through < 155.80 Mb. We emphasize that Line B mice are fully homozygous (HO) for NOD.B10 within the distal portion (155.80 through 157.36 Mb) of the 2008 narrowed *Aec2* disease susceptibility region [23] (see later Figure 3).

Cox-2flox **Line C** mice are derived from a still further recombination detected in the N7 generation of backcrossing to NOD.B10 (Table 1). These mice are uniformly NOD.B10 with the exception of a non-NOD region extending from > 144.18 Mb through < 155.19 Mb from the Chr 1 centromere. (Because fine mapping markers were not available, the non-NOD region maximally could include genes extending from > 139.52 Mb through < 155.80 Mb). We emphasize that Line C mice possess NOD alleles throughout both upstream and downstream sections of the 2008 narrowed *Aec2* region (D1Mit348 at 133.44 Mb through 139.52 Mb) [23] (see later Figure 3).

3.2 Salivation studies in Cox-2flox congenic Lines A, B, and C

Cox-2flox⁺ male mice of the N5 generation or greater were aged to at least 5 months (when NOD.B10 mice show high penetrance xerostomia, independently of gender [33]) and tested for saliva formation upon pilocarpine injection. Females and *Cox-2flox/flox* homozygous mice were additionally tested in later backcross generations.

Figure 2 shows that the first NOD.B10 *Cox-2flox* congenic strain developed, Line A, showed no signs of impaired salivation. The level of pilocarpine-induced salivation in aged Line A *Cox-2flox*⁺ male mice was significantly greater than that of age and sex-matched, disease-susceptible NOD.B10 wild-type mice ($p = 0.01$). Indeed, the amount of saliva generated from Line A mice was, if anything, greater than that of age and sex-matched C57BL/6 mice used as negative controls for xerostomia (borderline significance at $p = 0.06$). In contrast, as also illustrated in Figure 2, xerostomia was manifest in the two later NOD.B10 *Cox-2flox*⁺ congenic strains, Line B and Line C, and in *Cox-2flox/flox* homozygous Line B. The levels of pilocarpine-induced saliva in these latter lines were indistinguishable from that of wild-type NOD.B10 littermates.

3.3 Refinement of the Chr 1 Aec2 locus for SS xerostomia

Upon integrating genetic mapping of the above NOD.B10 *Cox-2flox* congenic lines (Table 1) with past insights on the upstream/downstream borders of the Chr 1 Aec2 locus [23], it becomes evident that loss of xerostomia in Line A mice can be attributed to a replacement of NOD alleles with 129 strain alleles throughout the above cited span of the Aec2 locus (Figure 3). Importantly, Figure 3 also shows that restored xerostomia in Line B and Line C mice represents regained NOD alleles only within a limited portion of the former mapped Aec2 locus. The latter is a span inclusive of rs33699657 (155.80 Mb from the Chr 1 centromere) through the end of the 2008-mapped Aec2 region at D1Mit268 (157.36 Mb) and is designated as “Region B” (Figure 3). Without more refined mapping, it is also possible that restored NOD alleles within a downstream region designated as “Region A” could contribute to regained disease. Region A contains genes of undetermined origin in Lines B and C (Figure 3) and extends from rs262568316 (155.19 Mb) to rs33699657 (155.80 Mb) on Chr 1.

3.4 Bioinformatics analysis of SNPs within protein-encoding genes in the narrowed Aec2 span

Table 2 provides a list of all protein-encoding genes within the above designated Aec2 subregions A and B. Genes *italicized* (with one asterisk) express SNP differences between the NOD and 129 mouse strains in either introns, RNA-UTR, and/or non-synonymous coding sequences, through bioinformatics analyses described in Section 2.2. Genes in ***bold italics*** (with two asterisks) represent those with at least one non-synonymous coding SNP that might alter protein function.

We wish to emphasize that the non-synonymous coding SNPs between NOD and the 129 strain do not reflect unique NOD mutations. Rather, NOD SNPs in the genes *Cep350*, *Tor1aip1*, *Tor1aip2*, *Tdrd5*, *Nphs2*, and *Axnd1* are shared with several other mouse strains that do not develop spontaneous SS upon aging, e.g. A/J, AKR/J, BALB/cJ, C3H/HeJ,

CBA/J and DBA/2J (as determined by the MPD database (<http://phenome.jax.org/>)). Furthermore, the non-synonymous coding SNPs that distinguish NOD and 129 within the genes for *Tor3a* and *Abl2* are shared between NOD and a differing set of mouse strains, e.g. C57BL/6J and C57BL/6NJ. Thus, the Chr 1 *Aec2* locus of NOD appears to represent a recombination between two major mouse lineages.

3.5 Evidence for sialadenitis (inflammatory foci within salivary glands) in all NOD.B10 *Cox-2flox* congenic strains

Infiltrates of mononuclear cells within salivary glands are quite characteristic of SS. Nevertheless, in both mice and humans, the extent of lymphocytic infiltration is not always concordant with clinical evidence of xerostomia [4, 36]. A similar lack of concordance was evidenced in this study. While NOD.B10 wt and congenic *Cox-2flox*⁺ Line A differed significantly in saliva output upon aging (Figure 2A), the submandibular salivary glands of nearly all examined mice showed evidence of sialadenitis (periductal leukocyte infiltration; *white arrows*) (Figure 4C: *Cox-2flox*⁺ Line A and Figure 4D and E: *Cox-2flox/flox* Line B). Given the limited numbers of *Cox-2flox*⁺ Line A mice available for study, we cannot eliminate the possibility that differences may have emerged with larger cohorts.

Figure 5 presents a quantitative comparison of the inflammatory infiltrates detected within the novel *Cox-2flox* congenic lines here studied, as compared to wild-type NOD.B10 controls. Regardless of whether measurements were made of the number of foci per submandibular lobe (Figure 5A), foci per mm² of gland (Figure 5B), or size of foci in mm² (Figure 5C), no significant differences were noted between NOD.B10 WT and NOD.B10 *Cox-2flox*⁺ Line A or *Cox-2flox*⁺ or *Cox-2flox/flox* Line B. At the time of the salivary gland study, adequately aged NOD.B10 *Cox-2flox* Line C mice were not available, but given that the latter have greater homology with NOD.B10 WT than do Line B, differences between Line C and WT are not anticipated. Of note, in both *Cox-2* WT and *Cox-2flox*⁺ Line B mice, a trend toward greater focal frequency in females over males was observed; however, this difference did not reach statistical significance.

4.0 DISCUSSION

In an effort to introduce a floxed *Cox-2* (*Ptgs2*) gene into the genetic background of SS-susceptible NOD.B10 mice, we have narrowed the candidate genes within Chr 1 which influence SS xerostomia in mice. Important to this development is the fact that the *Cox-2* gene resides within an earlier reported *Aec2* span [24].

Through genetic mapping of Chr 1 in *xerostomia-resistant* NOD.B10 *Cox-2flox*⁺ Line A mice, we confirmed an earlier report of Nguyen et al. that predisposing alleles resided within a region extending from 133.44 Mb (D1Mit348) through 157.36 Mb (D1Mit268) downstream of the Chr 1 centromere [23]. Nguyen et al. found this region important through breeding NOD susceptibility genes onto a non-susceptible C57BL/6 genetic background [23]. Conversely, we discerned its relevance by noting a loss of xerostomia when *Cox-2flox* and flanking genes (from non-susceptible mouse strain 129) were backcrossed onto the susceptible NOD.B10 background. The fact that this region was found critical through opposing approaches reinforces its relevance to SS. Furthermore, our finding that Line A

mice, which were heterozygous (HET) for *Cox-2flox*, manifest xerostomia-resistance showed that protection from this disease manifestation does not require homozygosity (HO) of the non-NOD alleles.

Of note, further fine genetic mapping of Chr 1 in the above Line A mice and in two later *xerostomia-susceptible* congenic lines enabled us to narrow the Chr 1 *Aec2* alleles affecting SS hyposalivation to a DNA region spanning 1.56 to 2.17 Mb on Chr 1. We excluded a relatively large segment from the above 2008-mapped *Aec2* locus [23]. The omitted segment maps from D1Mit348 (133.44 Mb) through rs262568316 (155.19 Mb) and includes the *Cox-2* gene which begins at 150.10 Mb. The basis for exclusion was evidence that both HET and HO *Cox-2flox* Line B mice (possessing non-NOD alleles in the latter span) developed SS xerostomia comparable to that noted in NOD.B10 wild-type mice. We want to emphasize the point that elimination of *Cox-2* and closely flanking genes as disease susceptibility genes (on the basis of alleles represented) *does not* mean that proteins encoded by these genes are irrelevant to SS. Rather, it means that there are no allelic differences which make one allele significantly more likely to cause this disease than another.

A possibility that cannot be presently precluded is that the above omitted span contains genes whose alleles influence the age at which xerostomia becomes manifest. Most of the mice here evaluated for xerostomia were substantially older than the past noted age threshold xerostomia development, ~ 17 to 24 months of age [37]. In their study of 39 recombinant inbred lines generated from crossing C57BL/6.NOD-*Aec1Aec2* mice with C57BL/6J mice, Nguyen et al. had suggested that quantitative trait loci (QTL) may be present at the centromeric end of their 2008-mapped *Aec2* locus [23].

The region presently defined as *Aec2 Region B* (between 155.80 Mb and 157.36 Mb) appears most likely to contain the Chr 1-localized genes whose alternative alleles strongly influence SS xerostomia. This conclusion is based on three factors: (a) past mapping which showed that the most downstream end of *Aec2* extends to D1Mit268 (157.36 Mb) [23]; (b) the current study's finding that Line A mice, which failed to develop xerostomia, lacked NOD-derived genes throughout Region B, whereas disease-susceptible Lines B and C possessed NOD alleles in this region; and (c) a bioinformatics search which showed that nearly all Region B protein-encoding genes express SNPs that distinguish the NOD and 129 mouse strains. Interestingly, of 16 protein-encoding genes in this region, 14 genes (88%) expressed differing SNPs in introns or RNA UTR regions and/or expressed non-synonymous coding SNPs. Eight genes (50%) displayed non-synonymous exon SNPs that could influence protein structure and /or function.

Region B genes with non-synonymous coding SNPs included *Cep350*, *Tor1aip1* (LAP), *Tor1aip2* (LULL1), *Tdrd5*, *Nphs2* (podocin), *Axdnd1*, *Abl2*, and *Tor3a*. ***Cep350*** is of particular interest in the context of SS. This gene encodes CAP350 [38], a centrosome- and microtubule-associating protein that is not extensively studied but is reported to directly engage and compartmentalize the PPAR group of nuclear hormone receptors, PPAR α and PPAR γ , within cell nuclei [39]. Interestingly, PPARs are linked to the COX-2/PGE2 axis [40] and known to strongly influence lipid metabolism, autoimmunity, and Th1 and Th17 subset development, in a sex-hormone-determined fashion [16, 41, 42]. CAP350

engagement with PPAR α was reported to sequester the latter in a subnuclear compartment and compromise its function as a transactivator [39]. Whether PPAR γ is similarly regulated is unknown. It will be of interest to compare the expression/function of CAP350 protein from NOD mice and SS-resistant mice expressing the diverse *Cep350* coding SNPs.

Another intriguing Region B gene found to manifest non-synonymous coding SNPs is *Tor3a* (also known as ADIR). In humans this gene is primarily expressed in salivary glands, lymph nodes, and stomach, but in mice its expression is more widespread [43]. The characterizations of *Tor3a* as an IFN- α -responsive gene [43], and SS as a disease with a strong IFN- α signature in both mice and humans [44, 45], suggest that *Tor3a* levels should be elevated in SS. Indeed, heightened levels of this protein are found in exosomes from human parotid gland saliva [46] as well as in PHA-activated T lymphoblasts, EBV-transformed B lymphoblasts and several B cell malignancies [47]. The *Tor3a* gene encodes an ER protein with 8 potential phosphorylation sites; coding SNPs might affect the potential for these modifications. Another intriguing attribute of *Tor3a* is its status as a minor histocompatibility molecule [47]. Conceivably, aspects of its structure could promote autologous T cell activation [48], particularly if triggering thresholds are altered by inflammatory changes within salivary gland tissues.

Five remaining genes within Region B with non-synonymous coding SNPs that distinguish NOD and 129 also warrant discussion. *Abl2*, encodes Arg, an F-actin-binding kinase that overlaps in function with Abl1, a related kinase with a critical role in lymphocyte development and signaling [49, 50]. *Tor1aip1* (LAP11) and *Tor1aip2* (LULL1), two neighboring genes, encode proteins which regulate the activity of Torsin A, an cytoplasmic ATPase [51, 52] that is linked to the nuclear skeleton, cell cycle, and lamins [53]. *Axdnd1* (axonemal dynein light chain domain containing 1) encodes a microtubule-binding protein with a role in intracellular transport. The two remaining genes with non-synonymous coding SNPs, *Tdrd5* (tudor domain containing 5) and *Nphs2* (podocin), appear less relevant to SS. *Nphs2* (podocin) is restricted to the kidney and *Tdrd5* is an RNA-binding protein thought to function primarily in maintaining germline integrity during spermatogenesis.

While not manifesting coding SNPs, three other Region B genes express intron and RNA-UTR SNPs that might affect mRNA synthesis, splicing and/or stability. The *Qsox1* gene encodes two major quiescin sulfhydryl oxidase 1 protein isoforms that are a consequence of differential RNA splicing. *Qsox1* proteins function in secretion, cell anchorage, and the regulation of cell oxidative stress and proliferation [54]; are present in salivary glands (<http://www.proteinatlas.org/ENSG00000116260/tissue>); and are elevated in certain malignancies [54]. *Soat1* is a sterol O-acyltransferase recently defined as a quantitative trait locus gene for hyperlipidemia [55] and was previously implicated as an *Aec2* lipid regulatory gene by Nguyen et al. on the basis of abnormal lipid accumulations in the salivary and lachrymal glands of SS-afflicted mice [23, 56]. Finally *Rasal2*, encodes a RasGAP family member which negatively regulates Ras function and whose deletion/mutation promotes tumor metastasis [57].

Although the additional *Aec2* span defined as *Region A* is located within the broad *Aec2* span mapped earlier by Nguyen et al. [23], the unavailability of fine mapping markers

precluded us from discerning whether alleles of Region A genes were of NOD or 129 origin. Bioinformatics analysis of the three protein-encoding genes present revealed that only one gene, *Acbd6*, expressed SNPs that distinguish NOD and 129. While the SNPs within this gene (encoding a cytoplasmic lipid, Acyl-CoA-binding protein [58]) do not affect exons, they might affect mRNA synthesis or stability.

Although the *Cox-2* gene possesses no SNPs that distinguish NOD and 129, the gene's location at the center of the *Aec2* disease susceptibility region [23] could be of significance. COX-2 is a critical modulator of PGE2 which, among its diverse functions, can mediate epigenetic changes through regulating the transcription of DNA methyltransferases, DNMT1, DNMT3a, and DNMT3b [59, 60]. Thus, there is an intriguing possibility that COX-2-regulated PGE2 influences the expression of proximal genes. Indeed, PGE2 has positive forward effects on *Cox-2* gene transcription [61, 62], but whether a change in the gene's methylation status [63] is involved is unclear. Other evidence that genes in physical proximity often show functional linkage and are co-transcribed [64, 65] is consistent with such a COX-2 regulatory role. The fact that many genes in the genetic block extending from 133.603 to 157.140 Mb of mouse Chr 1 show shared synteny between mice and humans (<http://www.animalgenome.org/Vcmap/>) suggests that there may be evolutionary pressure to retain their proximity.

In summary, through narrowing the *Aec2* span with a strong effect on xerostomia, this study has correspondingly narrowed the candidate disease susceptibility genes for this SS disease manifestation. Based on available information, we consider the most notable among these to be the genes encoding **CAP350**, a centriole and nucleus-associated protein that engages several members of the important PPAR nuclear receptor family; **Tor3a (ADIR)**, an IFN- α -upregulated protein which encodes a minor histocompatibility antigen expressed in normal salivary glands and activated lymphocytes; **Abl2 (Arg)**, an Abl1-related kinase; **Tor1aip1 (LAP11)** and **Tor1aip2 (LULL1)**, important regulatory proteins of the cytoplasmic ATPase, Torsin-A; and **Qsox1**, a salivary gland-expressed protein with roles in secretion, cell anchorage, proliferation, and regulation of oxidative stress. With better tools for resolving the importance of these genes and their products, and COX-2 as well, improved therapies to control a disorder afflicting millions of women over the age of 50 may be realized.

Acknowledgments

The authors gratefully acknowledge Yana Moses (Department of Pathology, North Shore LIJ Health System, NY) for assistance with tissue sectioning and H&E staining; Sarah Reutzel for executing all the MAX-BAX® testing and fine mapping; Hyunjoo Lee for her early assistance in the mouse genome bioinformatics analysis; Philip Chum for help with salivation analyses; and Dr. Percio Gulko for useful discussions and review of the manuscript. Support for this project came from the Sjogren's Syndrome Foundation (Innovative Concept Award to PKAM) and NIH NIAMS R21 AR061653 (to PKAM) and Feinstein Center for CLL Research funds from Dr. Nicholas Chiorazzi.

Abbreviations

(BCR) B cell antigen receptor

(HET)	Cyclooxygenase-2 (<i>Cox-2</i> = gene; COX-2 = protein) Heterozygous
(HO)	Homozygous
(MGD)	Mouse Genome Database
(MPD)	Mouse Phenome Database
(PGE2)	Nuclear localization sequence (NLS) Prostaglandin E2
(SNP)	Single nucleotide polymorphism
(SS)	Sjogren's syndrome

REFERENCES

- [1]. Voulgarelis M, Tzioufas AG. Pathogenetic mechanisms in the initiation and perpetuation of Sjogren's syndrome. *Nat Rev Rheumatol*. 2010; 6:529–37. [PubMed: 20683439]
- [2]. Ekstrom Smedby K, Vajdic CM, Falster M, Engels EA, Martinez-Maza O, Turner J, et al. Autoimmune disorders and risk of non-Hodgkin lymphoma subtypes: a pooled analysis within the InterLymph Consortium. *Blood*. 2008; 111:4029–38. [PubMed: 18263783]
- [3]. Mariette X, Roux S, Zhang J, Bengoufa D, Lavie F, Zhou T, et al. The level of BLYS (BAFF) correlates with the titre of autoantibodies in human Sjogren's syndrome. *Ann Rheum Dis*. 2003; 62:168–71. [PubMed: 12525388]
- [4]. Nguyen CQ, Gao JH, Kim H, Saban DR, Cornelius JG, Peck AB. IL-4-STAT6 signal transduction-dependent induction of the clinical phase of Sjogren's syndrome-like disease of the nonobese diabetic mouse. *J Immunol*. 2007; 179:382–90. [PubMed: 17579059]
- [5]. Robinson CP, Brayer J, Yamachika S, Esch TR, Peck AB, Stewart CA, et al. Transfer of human serum IgG to nonobese diabetic Igmu null mice reveals a role for autoantibodies in the loss of secretory function of exocrine tissues in Sjogren's syndrome. *Proc Natl Acad Sci U S A*. 1998; 95:7538–43. [PubMed: 9636185]
- [6]. St Clair EW, Levesque MC, Prak ET, Vivino FB, Alappatt CJ, Szychala ME, et al. Rituximab therapy for primary Sjogren's syndrome: an open-label clinical trial and mechanistic analysis. *Arthritis Rheum*. 65:1097–106. [PubMed: 23334994]
- [7]. Salomonsson S, Jonsson MV, Skarstein K, Brokstad KA, Hjelmstrom P, Wahren-Herlenius M, et al. Cellular basis of ectopic germinal center formation and autoantibody production in the target organ of patients with Sjogren's syndrome. *Arthritis Rheum*. 2003; 48:3187–201. [PubMed: 14613282]
- [8]. Huang YF, Cheng Q, Jiang CM, An S, Xiao L, Gou YC, et al. The immune factors involved in the pathogenesis, diagnosis, and treatment of Sjogren's syndrome. *Clin Dev Immunol*. 2013:160491. [PubMed: 23935646]
- [9]. Gao J, Killedar S, Cornelius JG, Nguyen C, Cha S, Peck AB. Sjogren's syndrome in the NOD mouse model is an interleukin-4 time-dependent, antibody isotype-specific autoimmune disease. *J Autoimmun*. 2006; 26:90–103. [PubMed: 16413168]
- [10]. Cha S, Singson E, Cornelius J, Yagna JP, Knot HJ, Peck AB. Muscarinic acetylcholine type-3 receptor desensitization due to chronic exposure to Sjogren's syndrome-associated autoantibodies. *J Rheumatol*. 2006; 33:296–306. [PubMed: 16465661]
- [11]. Tsuboi H, Matsumoto I, Wakamatsu E, Nakamura Y, Iizuka M, Hayashi T, et al. New epitopes and function of anti-M3 muscarinic acetylcholine receptor antibodies in patients with Sjogren's syndrome. *Clin Exp Immunol*. 2010; 162:53–61. [PubMed: 20731676]
- [12]. Dawson LJ, Stanbury J, Venn N, Hasdimir B, Rogers SN, Smith PM. Antimuscarinic antibodies in primary Sjogren's syndrome reversibly inhibit the mechanism of fluid secretion by human submandibular salivary acinar cells. *Arthritis Rheum*. 2006; 54:1165–73. [PubMed: 16572451]

- [13]. Nguyen CQ, Hu MH, Li Y, Stewart C, Peck AB. Salivary gland tissue expression of interleukin-23 and interleukin-17 in Sjogren's syndrome: findings in humans and mice. *Arthritis Rheum.* 2008; 58:734–43. [PubMed: 18311793]
- [14]. Park H, Li Z, Yang XO, Chang SH, Nurieva R, Wang YH, et al. A distinct lineage of CD4 T cells regulates tissue inflammation by producing interleukin 17. *Nat Immunol.* 2005; 6:1133–41. [PubMed: 16200068]
- [15]. Mitsdoerffer M, Lee Y, Jager A, Kim HJ, Korn T, Kolls JK, et al. Proinflammatory T helper type 17 cells are effective B-cell helpers. *Proc Natl Acad Sci U S A.* 2010; 107:14292–7. [PubMed: 20660725]
- [16]. Zhang MA, Rego D, Moshkova M, Kebir H, Chruscinski A, Nguyen H, et al. Peroxisome proliferator-activated receptor (PPAR)alpha and -gamma regulate IFNgamma and IL-17A production by human T cells in a sex-specific way. *Proc Natl Acad Sci U S A.* 109:9505–10. [PubMed: 22647601]
- [17]. Bettelli E, Carrier Y, Gao W, Korn T, Strom TB, Oukka M, et al. Reciprocal developmental pathways for the generation of pathogenic effector TH17 and regulatory T cells. *Nature.* 2006; 441:235–8. [PubMed: 16648838]
- [18]. Khayrullina T, Yen JH, Jing H, Ganea D. In vitro differentiation of dendritic cells in the presence of prostaglandin E2 alters the IL-12/IL-23 balance and promotes differentiation of Th17 cells. *J Immunol.* 2008; 181:721–35. [PubMed: 18566439]
- [19]. Yao C, Sakata D, Esaki Y, Li Y, Matsuoka T, Kuroiwa K, et al. Prostaglandin E2-EP4 signaling promotes immune inflammation through Th1 cell differentiation and Th17 cell expansion. *Nat Med.* 2009; 15:633–40. [PubMed: 19465928]
- [20]. Boniface K, Bak-Jensen KS, Li Y, Blumenschein WM, McGeachy MJ, McClanahan TK, et al. Prostaglandin E2 regulates Th17 cell differentiation and function through cyclic AMP and EP2/EP4 receptor signaling. *J Exp Med.* 2009; 206:535–48. [PubMed: 19273625]
- [21]. Lessard CJ, Li H, Adrianto I, Ice JA, Rasmussen A, Grundahl KM, et al. Variants at multiple loci implicated in both innate and adaptive immune responses are associated with Sjogren's syndrome. *Nat Genet.* 45:1284–92. [PubMed: 24097067]
- [22]. Cha S, Nagashima H, Brown VB, Peck AB, Humphreys-Beher MG. Two NOD Idd-associated intervals contribute synergistically to the development of autoimmune exocrinopathy (Sjogren's syndrome) on a healthy murine background. *Arthritis Rheum.* 2002; 46:1390–8. [PubMed: 12115247]
- [23]. Nguyen CQ, Cornelius JG, Cooper L, Neff J, Tao J, Lee BH, et al. Identification of possible candidate genes regulating Sjogren's syndrome-associated autoimmunity: a potential role for TNFSF4 in autoimmune exocrinopathy. *Arthritis Res Ther.* 2008; 10:R137. [PubMed: 19032782]
- [24]. Nguyen C, Singson E, Kim JY, Cornelius JG, Attia R, Doyle ME, et al. Sjogren's syndrome-like disease of C57BL/6.NOD-Aec1 Aec2 mice: gender differences in keratoconjunctivitis sicca defined by a cross-over in the chromosome 3 Aec1 locus. *Scand J Immunol.* 2006; 64:295–307. [PubMed: 16918699]
- [25]. Ryan EP, Malboeuf CM, Bernard M, Rose RC, Phipps RP. Cyclooxygenase-2 inhibition attenuates antibody responses against human papillomavirus-like particles. *J Immunol.* 2006; 177:7811–9. [PubMed: 17114452]
- [26]. Roper RL, Phipps RP. Prostaglandin E2 and cAMP inhibit B lymphocyte activation and simultaneously promote IgE and IgG1 synthesis. *J Immunol.* 1992; 149:2984–91. [PubMed: 1328389]
- [27]. Mongini PK, Inman JK, Han H, Fattah RJ, Abramson SB, Attur M. APRIL and BAFF promote increased viability of replicating human B2 cells via mechanism involving cyclooxygenase 2. *J Immunol.* 2006; 176:6736–51. [PubMed: 16709833]
- [28]. Lee H, Trott JS, Haque S, McCormick S, Chiorazzi N, Mongini PK. A cyclooxygenase-2/prostaglandin E2 pathway augments activation-induced cytosine deaminase expression within replicating human B cells. *J Immunol.* 2010; 185:5300–14. [PubMed: 20921530]
- [29]. Ishikawa TO, Herschman HR. Conditional knockout mouse for tissue-specific disruption of the cyclooxygenase-2 (Cox-2) gene. *Genesis.* 2006; 44:143–9. [PubMed: 16496341]

- [30]. Narasimha AJ, Watanabe J, Ishikawa TO, Priceman SJ, Wu L, Herschman HR, et al. Absence of myeloid COX-2 attenuates acute inflammation but does not influence development of atherosclerosis in apolipoprotein E null mice. *Arterioscler Thromb Vasc Biol.* 2010; 30:260–8. [PubMed: 19926832]
- [31]. Wong GT. Speed congenics: applications for transgenic and knock-out mouse strains. *Neuropeptides.* 2002; 36:230–6. [PubMed: 12359513]
- [32]. Eppig JT, Blake JA, Bult CJ, Kadin JA, Richardson JE. The Mouse Genome Database (MGD): comprehensive resource for genetics and genomics of the laboratory mouse. *Nucleic Acids Res.* 40:D881–6. [PubMed: 22075990]
- [33]. Robinson CP, Yamachika S, Bounous DI, Brayer J, Jonsson R, Holmdahl R, et al. A novel NOD-derived murine model of primary Sjogren's syndrome. *Arthritis Rheum.* 1998; 41:150–6. [PubMed: 9433880]
- [34]. Deshmukh US, Ohyama Y, Bagavant H, Guo X, Gaskin F, Fu SM. Inflammatory stimuli accelerate Sjogren's syndrome-like disease in (NZB x NZW)F1 mice. *Arthritis Rheum.* 2008; 58:1318–23. [PubMed: 18438852]
- [35]. Vitali C, Bombardieri S, Jonsson R, Moutsopoulos HM, Alexander EL, Carsons SE, et al. Classification criteria for Sjogren's syndrome: a revised version of the European criteria proposed by the American-European Consensus Group. *Ann Rheum Dis.* 2002; 61:554–8. [PubMed: 12006334]
- [36]. Nguyen CQ, Peck AB. Unraveling the pathophysiology of Sjogren syndrome-associated dry eye disease. *Ocul Surf.* 2009; 7:11–27. [PubMed: 19214349]
- [37]. Jonsson MV, Delaleu N, Brokstad KA, Berggreen E, Skarstein K. Impaired salivary gland function in NOD mice: association with changes in cytokine profile but not with histopathologic changes in the salivary gland. *Arthritis Rheum.* 2006; 54:2300–5. [PubMed: 16802370]
- [38]. Hoppeler-Lebel A, Celati C, Bellett G, Mogensen MM, Klein-Hitpass L, Bornens M, et al. Centrosomal CAP350 protein stabilises microtubules associated with the Golgi complex. *J Cell Sci.* 2007; 120:3299–308. [PubMed: 17878239]
- [39]. Patel H, Truant R, Rachubinski RA, Capone JP. Activity and subcellular compartmentalization of peroxisome proliferator-activated receptor alpha are altered by the centrosome-associated protein CAP350. *J Cell Sci.* 2005; 118:175–86. [PubMed: 15615782]
- [40]. Aleshin S, Strokin M, Sergeeva M, Reiser G. Peroxisome proliferator-activated receptor (PPAR)beta/delta, a possible nexus of PPARalpha- and PPARgamma-dependent molecular pathways in neurodegenerative diseases: Review and novel hypotheses. *Neurochem Int.* 63:322–30. [PubMed: 23811400]
- [41]. Choi JM, Bothwell AL. The nuclear receptor PPARs as important regulators of T-cell functions and autoimmune diseases. *Mol Cells.* 33:217–22. [PubMed: 22382683]
- [42]. Dunn SE, Ousman SS, Sobel RA, Zuniga L, Baranzini SE, Youssef S, et al. Peroxisome proliferator-activated receptor (PPAR)alpha expression in T cells mediates gender differences in development of T cell-mediated autoimmunity. *J Exp Med.* 2007; 204:321–30. [PubMed: 17261635]
- [43]. Dron M, Meritet JF, Dandoy-Dron F, Meyniel JP, Maury C, Tovey MG. Molecular cloning of ADIR, a novel interferon responsive gene encoding a protein related to the torsins. *Genomics.* 2002; 79:315–25. [PubMed: 11863361]
- [44]. Nordmark G, Alm GV, Ronnblom L. Mechanisms of Disease: primary Sjogren's syndrome and the type I interferon system. *Nat Clin Pract Rheumatol.* 2006; 2:262–9. [PubMed: 16932699]
- [45]. Nguyen CQ, Peck AB. The Interferon-Signature of Sjogren's Syndrome: How Unique Biomarkers Can Identify Underlying Inflammatory and Immunopathological Mechanisms of Specific Diseases. *Front Immunol.* 4:142. [PubMed: 23847613]
- [46]. Gonzalez-Begne M, Lu B, Han X, Hagen FK, Hand AR, Melvin JE, et al. Proteomic analysis of human parotid gland exosomes by multidimensional protein identification technology (MudPIT). *J Proteome Res.* 2009; 8:1304–14. [PubMed: 19199708]
- [47]. van Bergen CA, Kester MG, Jedema I, Heemskerk MH, van Luxemburg-Heijs SA, Kloosterboer FM, et al. Multiple myeloma-reactive T cells recognize an activation-induced minor

- histocompatibility antigen encoded by the ATP-dependent interferon-responsive (ADIR) gene. *Blood*. 2007; 109:4089–96. [PubMed: 17234742]
- [48]. Glimcher LH, Longo DL, Green I, Schwartz RH. Murine syngeneic mixed lymphocyte response. I. Target antigens are self Ia molecules. *J Exp Med*. 1981; 154:1652–70. [PubMed: 6170721]
- [49]. Gu JJ, Ryu JR, Pendergast AM. Abl tyrosine kinases in T-cell signaling. *Immunol Rev*. 2009; 228:170–83. [PubMed: 19290927]
- [50]. Liberatore RA, Goff SP. c-Abl-deficient mice exhibit reduced numbers of peritoneal B-1 cells and defects in BCR-induced B cell activation. *Int Immunol*. 2009; 21:403–14. [PubMed: 19228876]
- [51]. Zhao C, Brown RS, Chase AR, Eisele MR, Schlieker C. Regulation of Torsin ATPases by LAP1 and LULL1. *Proc Natl Acad Sci U S A*. 110:E1545–54. [PubMed: 23569223]
- [52]. Goodchild RE, Dauer WT. The AAA+ protein torsinA interacts with a conserved domain present in LAP1 and a novel ER protein. *J Cell Biol*. 2005; 168:855–62. [PubMed: 15767459]
- [53]. Simon DN, Wilson KL. The nucleoskeleton as a genome-associated dynamic ‘network of networks’. *Nat Rev Mol Cell Biol*. 12:695–708. [PubMed: 21971041]
- [54]. Katchman BA, Ocal IT, Cunliffe HE, Chang YH, Hostetter G, Watanabe A, et al. Expression of quiescin sulfhydryl oxidase 1 is associated with a highly invasive phenotype and correlates with a poor prognosis in Luminal B breast cancer. *Breast Cancer Res*. 15:R28. [PubMed: 23536962]
- [55]. Lu Z, Yuan Z, Miyoshi T, Wang Q, Su Z, Chang CC, et al. Identification of Soat1 as a quantitative trait locus gene on mouse chromosome 1 contributing to hyperlipidemia. *PLoS One*. 6:e25344. [PubMed: 22022387]
- [56]. Nguyen CQ, Sharma A, She JX, McIndoe RA, Peck AB. Differential gene expressions in the lacrimal gland during development and onset of keratoconjunctivitis sicca in Sjogren’s syndrome (SJS)-like disease of the C57BL/6.NOD-Aec1Aec2 mouse. *Exp Eye Res*. 2009; 88:398–409. [PubMed: 19103199]
- [57]. McLaughlin SK, Olsen SN, Dake B, De Raedt T, Lim E, Bronson RT, et al. The RasGAP gene, RASAL2, is a tumor and metastasis suppressor. *Cancer Cell*. 24:365–78. [PubMed: 24029233]
- [58]. Soupene E, Serikov V, Kuypers FA. Characterization of an acyl-coenzyme A binding protein predominantly expressed in human primitive progenitor cells. *J Lipid Res*. 2008; 49:1103–12. [PubMed: 18268358]
- [59]. Huang SK, Scruggs AM, Donaghy J, McEachin RC, Fisher AS, Richardson BC, et al. Prostaglandin E(2) increases fibroblast gene-specific and global DNA methylation via increased DNA methyltransferase expression. *FASEB J*. 2012; 26:3703–14. [PubMed: 22645246]
- [60]. Xia D, Wang D, Kim SH, Katoh H, DuBois RN. Prostaglandin E2 promotes intestinal tumor growth via DNA methylation. *Nat Med*. 2012; 18:224–6. [PubMed: 22270723]
- [61]. Ishikawa TO, Jain N, Herschman HR. Feedback regulation of cyclooxygenase-2 transcription *ex vivo* and *in vivo*. *Biochem Biophys Res Commun*. 2009; 378:534–8. [PubMed: 19061862]
- [62]. Steinert D, Kuper C, Bartels H, Beck FX, Neuhofer W. PGE2 potentiates tonicity-induced COX-2 expression in renal medullary cells in a positive feedback loop involving EP2-cAMP-PKA signaling. *Am J Physiol Cell Physiol*. 2009; 296:C75–87. [PubMed: 19005164]
- [63]. Toyota M, Shen L, Ohe-Toyota M, Hamilton SR, Sinicrope FA, Issa JP. Aberrant methylation of the Cyclooxygenase 2 CpG island in colorectal tumors. *Cancer Res*. 2000; 60:4044–8. [PubMed: 10945606]
- [64]. Eisen MB, Spellman PT, Brown PO, Botstein D. Cluster analysis and display of genome-wide expression patterns. *Proc Natl Acad Sci U S A*. 1998; 95:14863–8. [PubMed: 9843981]
- [65]. Dottorini T, Palladino P, Senin N, Persampieri T, Spaccapelo R, Crisanti A. CluGene: A Bioinformatics Framework for the Identification of Co-Localized, Co-Expressed and Co-Regulated Genes Aimed at the Investigation of Transcriptional Regulatory Networks from High-Throughput Expression Data. *PLoS One*. 8:e661962.

HIGHLIGHTS

- SS-susceptible NOD.B10 mice with a floxed *Cox2* (*Ptgs2*) gene in Chr 1 are identified
- Candidate Chr 1 *Aec2* genes affecting SS hyposalivation (xerostomia) are narrowed
- Susceptibility alleles are downstream of *Ptgs2* and within a 1.56 to 2.17 Mb span of DNA
- Narrowed *Aec2* span contains 8 genes with non-synonymous coding SNPs
- The latter genes encode proteins with roles in immunity and cell proliferation

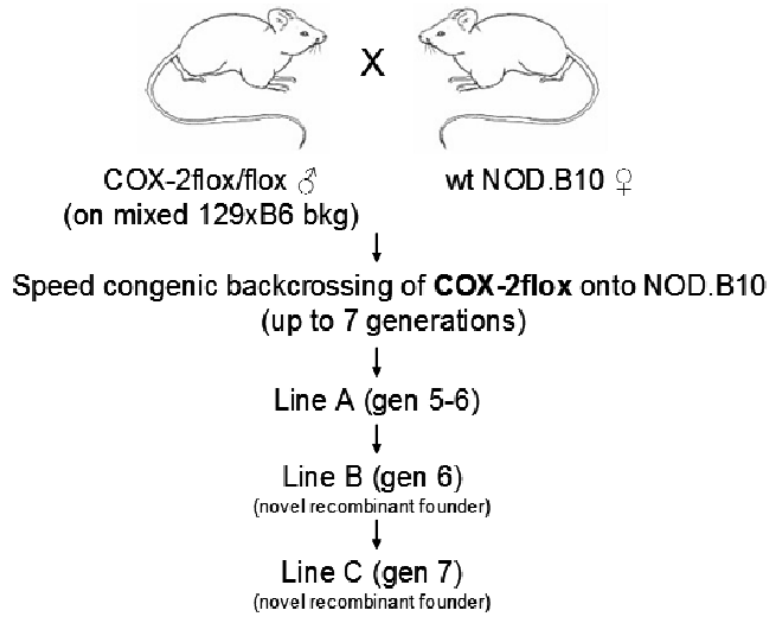


FIGURE 1. Schematic for development of NOD.B10 congenic mouse lines expressing *Cox-2flox* MAX-BAX® speed congenic breeding was used to backcross a *Cox-2flox* gene onto the NOD.B10 genetic background (Section 2.1). Line A *Cox-2flox*/+ mice tested below for salivation and sialadenitis derived from the 5th and 6th backcross generation; Tested Line B *Cox-2flox*/+ and *Cox-2flox/flox* mice were derived from an F1 cross between the *Cox-2flox*/+ heterozygous offspring of the 6th backcross generation. Tested Line C *Cox-2flox*/+ mice were derived from an F1 cross of the heterozygous offspring from an 8th backcross generation.

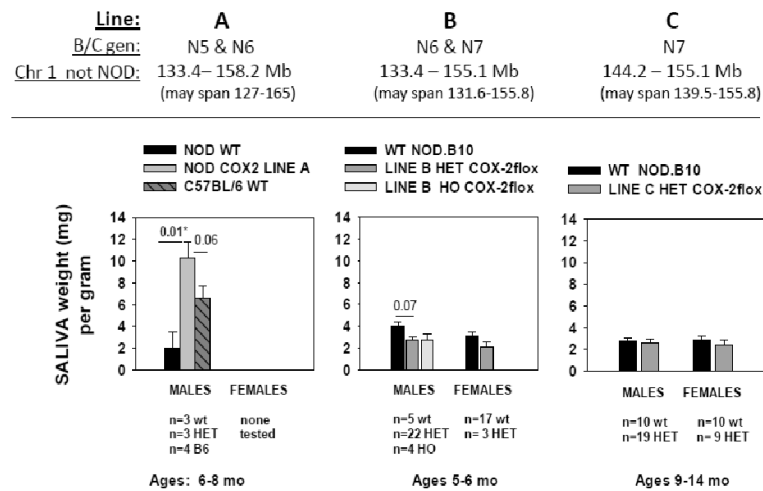


FIGURE 2. Aged NOD.B10 *Cox-2floX/+* Line A mice do not manifest hyposalivation (xerostomia), while aged *Cox-2floX/+* and *Cox-2floX/floX* Line B and *Cox-2floX/+* Line C mice do As aged mice of NOD.B10 *Cox-2floX* Lines A, B, and C became available throughout the backcrossing process, they were tested for salivation by i.p. injection of pilocarpine, a non-selective muscarinic receptor agonist. In testing Line A, comparisons were made to both age and sex matched NOD.B10 wild-type mice (+ control for xerostomia) and C57BL/6 mice (neg control for xerostomia). In later examination of Lines B and C, comparisons were made to age and sex-matched backcross littermates which did not express the *Cox-2floX* gene. HET = heterozygosity for *Cox-2floX*; HO = homozygosity for *Cox-2floX*; WT = wild-type NOD.B10 for *Cox-2*. Plotted values represent amount of saliva obtained (mean weight in mg \pm SEM) within each group. P values of statistical significance (<0.05) are indicated by an asterisk. The findings that saliva levels in Line A were significantly greater than NOD.B10 WT mice, and even exceeded levels in negative control C57BL/6 mice (albeit not at a level of statistical significance) indicate that Line A lacks the *Aec2* alleles needed for development of SS xerostomia. The finding that the saliva levels measured in Line B mice (HET and HO) are not significantly different from NOD.B10 *Cox-2* WT littermates indicates that genes spanning the region 134.2 to 153.7 Mb from the Chr 1 centromere *do not* display allelic differences that control the development of SS xerostomia.

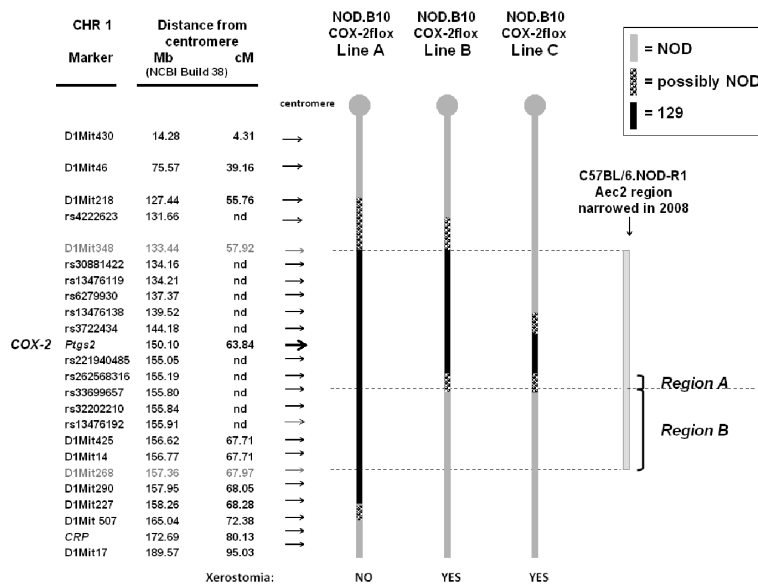
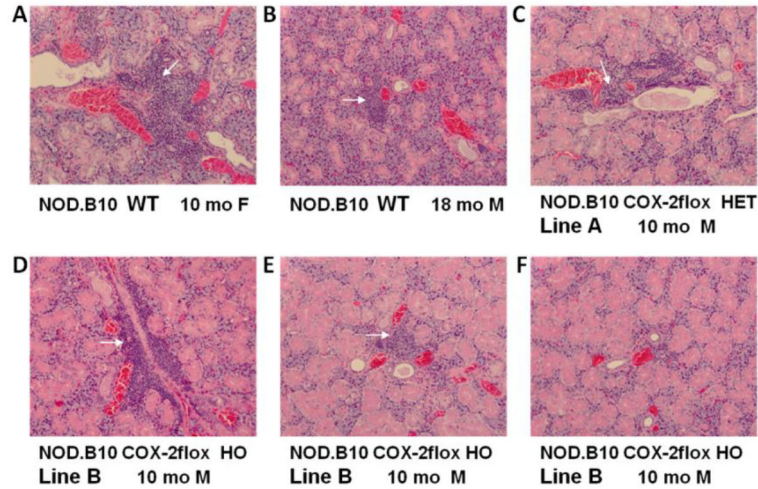


FIGURE 3. Schematic of regions of recombination in mouse chromosome 1 within novel NOD.B10 *Cox-2flox* congenic lines developed by backcrossing *Coxflox* onto SS-susceptible NOD.B10 genetic background

The major Chr 1 mapping markers used for fine mapping are shown, as well as their location in cM or as Mb from the Chr 1 centromere (based on recent NCBI Build 38 [32]). Regions mapping definitively as NOD genotype are shown in *grey*; regions with genes that are definitively not-NOD are shown in *black*; regions of unknown origin are shown *hatched*. The bar to the right shows the span of the *Aec2* locus, as mapped in 2008 by Nguyen et al. [23]. The salivation assessments of Lines A, B, and C in Figure 2 show that allelic differences in genes spanning 133.44 to 155.19 Mb do not determine SS disease susceptibility in mice. Region B likely contains SS pre-disposing alleles and Region A may as well. These SS candidate alleles are listed in Table 2.



H&E stained submandibular glands
(original magnification = 200x).

FIGURE 4. Periductal leukocyte infiltrates are present within salivary glands of aged *Cox-2flox*/+ (HET) Line A mice (no xerostomia) and *Cox-2flox*/+ and *Cox-2flox/flox* (HO) Line B mice (with xerostomia)

Submandibular salivary glands were excised from aged NOD.B10 wild-type male (M) and female (F) mice, as well as male mice of congenic *Cox-2flox* Line A or Line B. Tissue was immediately fixed and paraffin-embedded. Sliced, H&E stained tissues were viewed and photographed at an original magnification of 200X. In each case, an effort was made to photograph a section containing a typical infiltrate (shown by white arrows). The section in F, representing a salivary gland from a Line B homozygous (HO) mouse did not exhibit any foci, whereas foci were clearly evidenced in Line B HO mice shown in D and E.

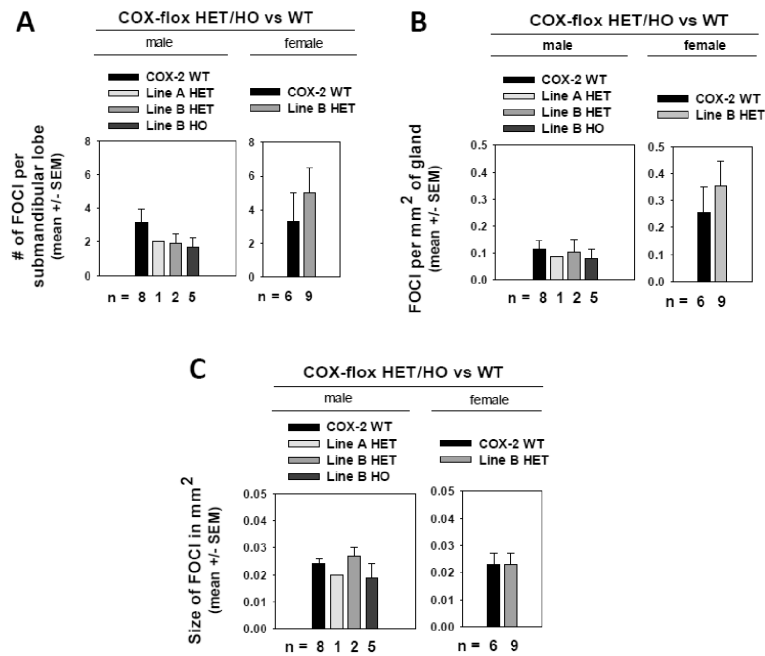


FIGURE 5. Neither frequency nor size of leukocytic foci differ significantly between aged NOD.B10 wild-type mice and congenic NOD.B10 *Cox-2flox/+* or *Cox-2flox/flox* Line B mice Efforts were made to quantify sialadenitis in the mice under study through comparisons of (A) the number of foci per submandibular lobe; (B) the number of foci per mm² of gland and (C) the size of each infiltrate in mm². Shown are the mean \pm SEM values for mice of each group. In the case of NOD.B10 *Cox-2flox/+* Line A, values for the single mouse (10 mo of age) are shown. Values for all NOD.B10 WT were pooled according to gender; ages of the males and females at the time of salivary gland excision ranged from 8-18 months (males) and 8-10 months (females). Salivary glands from congenic *Cox-2flox* line B mice were obtained at the following ages: flox/+ HET males (5-8 mo); flox/flox HO males (8 mo); and HET females (10 mo). (Note: in measuring size, infiltrates were not reliably measured if they were less than 0.01 mm². For the purposes of calculation, the latter were nevertheless given a score of 0.01, and this may have slightly inflated the average size of infiltrates.) Statistical analyses indicated no significant statistical difference between any test group and its respective WT, within each gender group.

Table 1

Mapping of CHR 1 recombination sites in NOD.B10 COX-2flox congenic lines

CHR	Marker ID	cM	Mb (NCBI Build 36)	N5 GENERATION		N6 GENERATION		N7 GENERATION	
				LINE A		LINE A	LINE B	LINE B	LINE C
1	D1Mit430 to D1Mi46	4.3 -39.16	14.28 -75.57	NOD		NOD	NOD	NOD	NOD
1	D1Mit308	50.78	110.60	NOD		NOD	NOD	NOD	NOD
1	D1Mit218	55.76	127.44	NOD		NOD	NOD	NOD	NOD
1	rs4222623		131.96				NOD	NOD	
1	D1Mit348	57.92	133.44				129	NOD	
1	rs30881422		134.16				129	NOD	
1	rs30882302		134.19				129	NOD	
1	rs13476119		134.21				129	NOD	
1	rs13476121		134.67				129	NOD	
1	rs6279930		137.37				129	NOD	
1	rs13476138		139.52				129	NOD	
1	rs3722434		144.18				129	129	
1	D1Mit102	63.32	147.24	129		129	129	129	129
<i>1</i>	<i>Ptgs-2-flox</i>	63.84	150.10	129		129	129	129	129
1	D1Mit501	64.93	152.62	129		129	129	129	129
1	D1Mit396	65.26	153.12				129	129	
1	D1Mit104	65.42	153.68				129	129	
1	rs13476185		153.71				129	129	
1	rs221940485		155.05				129	129	
1	rs262568316		155.19				129	129	
1	rs33699657		155.80				NOD	NOD	
1	rs32202210		155.84				NOD	NOD	
1	D1Mit451	67.67	155.96	129		129	NOD	NOD	NOD
1	D1Mit425	67.71	156.62	129		129	NOD	NOD	NOD
1	D1Mit14	67.71	156.77			129			
1	D1Mit290	68.05	157.95			129			
1	D1Mit227	68.028	158.26			129			
1	D1Mit507	72.38	165.04	NOD		NOD	NOD	NOD	NOD
1	CRP	80.13	172.69	NOD		NOD	NOD	NOD	NOD
1	D1Mit362	94.35	189.25	NOD		NOD	NOD	NOD	NOD
1	D1Mit17	95.03	189.57	NOD		NOD	NOD	NOD	NOD

^aN5 generation mice were fully NOD in all other chromosomes (> 99% congenic) on the basis of full autosomal chromosome screen with micorsatellite markers.

Table 2

Protein-encoding genes encoded within presently narrowed Aec2 sub-regions in Chr 1

	Mb from centromere ^a	Gene
	155.275	Xpr1, xenotropic and polytropic retrovirus receptor 1
Region A	155.558 *	<i>Acbd6</i> , acyl-Coenzyme A binding domain containing 6
	155.698	Lhx4, LIM homeobox protein 4
	155.778 *	<i>Qsox1</i> , quiescin Q6 sulfhydryl oxidase 1
	155.844 **	<i>Cep350</i> , centrosomal protein 350 (CAP350)
	156.006 **	<i>Tor1aip1</i> , torsin A interacting protein 1 (LAP1)
	156.035 **	<i>Tor1aip2</i> , torsin A interacting protein 2 (LULL1)
	156.075	Fam163a, family with sequence similarity 163, member A
	156.255 **	<i>Tdrd5</i> , tudor domain containing 5
	156.310 **	<i>Nphs2</i> , nephrosis 2 homolog, podocin (human)
Region B	156.323 **	<i>Axdnd1</i> , axonemal dynein light chain domain containing 1
	156.428 *	<i>Soat1</i> , sterol O-acyltransferase 1
	156.558 ** ^d	<i>Abl2</i> , Abelson murine leukemia viral oncogene homolog 2
	156.653 **	<i>Tor3a</i> , torsin family 3, member A (ADIR)
	156.678 *	<i>Fom20b</i> , family with sequence similarity 20, member B
	156.804 *	<i>Rolgps2</i> , Ral GEF with PH domain and SH3 binding motif 2
	156.838 *	<i>Angptl1</i> , angiopoietin-like 1
	157.099	Tex35, testis expressed 35
	157.140 *	<i>Rosal2</i> , RAS protein activator like 2

^a Chr 1 position based on GRCm36 genome coordinates (MGD database: (URL: <http://www.informatics.jax.org>) [Nov 2013])

^b One asterisk and *italics* indicates SNP differences between NOD and 129 in introns and/or RNA-UTR, as determined by the MGD mouse SNP database above.

^c Two asterisks and *bold italics* indicates that in addition to the above SNP differences, the gene displays one or more non-synonymous coding SNP differences between NOD & 129.

^d An *Abl2* gene non-synonymous coding SNP (rs30466582) is reported in the MPD, but not MGD database.